IChemE
www.icheme.org/journals
doi: 10.1205/cherd.04157

0263–8762/05/$30.00+0.00

Trans IChemE, Part A, February 2005
Chemical Engineering Research and Design, 83(A2): 153–159

CONTROL STRUCTURE DESIGN FOR PARALLEL PROCESSES Application to Heat-integrated Distillation

W.-H. TSAI, H.-P. HUANG and C.-C. YU*

Department of Chemical Engineering, National Taiwan University, Taipei, Taiwan

Parallel process units are often encountered in chemical process systems for different considerations, e.g., parallel reactors from reactor network synthesis, parallel columns for heat integration. One notable example is the feed split configuration of heat-integrated distillation columns. In this work, the control of parallel processes is illustrated with the heat-integrated distillation column example. Results show that more consistent control performance can be achieved using the proposed control structure for both feed composition and feed flow disturbances. More importantly, the improvement is obtained using simpler instrumentation and much less engineering effort.

Keywords: heat-integration; distillation configuration; parallel process; control structure design.

INTRODUCTION

Parallel process units are often encountered in chemical process systems for different considerations, e.g., parallel reactors from reactor network synthesis, parallel columns for heat integration. On the production plant level, we have seen parallel production lines for the same product. On the unit operation level, one notable example is the feed split configuration of heat-integrated distillation column (King, 1980; Chiang and Luyben, 1983; Andrecovich and Westerberg, 1985) where the feed is splitted into two streams and are fed separately to two columns which are heat-integrated, theoretically 50% energy can be saved by parallelizing the process. This unique process configuration, in theory, will lead to somewhat different control structure design, because we are interested in the global product quality measure (instead of the local one). In other words, one should take advantage of the process configuration to devise simpler and yet effective control structure.

We have seen extensive literature on the design and control of heat-integrated distillation systems. Tyreus and Luyben (1976) examine the control issue of double-effect distillation and an auxiliary reboiler is suggested for improved control performance. Chiang and Luyben (1988) study the control for three different heat-integration configurations: feed-split, light-split forward (integration), and light-split reverse. They concluded that the light-split reverse is the most controllable scheme. Weitz and Lewin (1996) study the same system using the disturbance cost as a controllability measure and a similar conclusion is drawn. Wang and Lee (2002) explore nonlinear PI control for binary high-purity heat-integrated columns with light split/reverse configuration. Yang *et al.* (2000) use a simplified model derived from state space equations to evaluate disturbance propagation for double-effect column under feed-split configuration.

Interaction between design and control for heat-integrated and/or thermally coupled distillation systems are studied by Rix and Gelbe (2000) and Bildea and Dimian (1999) using dynamic RGA as a controllability measure. Lin and Yu (2004) explore the interaction between design and control for heat-integrated columns. However, few of these works take advantage of the parallel characteristic of the processes into account. That is, in control structure design, one should emphasize on the output of the entire system instead of the output of individual (parallel) unit. The objective of this work is to explore the design and control of parallel processes and it is illustrated using heat-integrated distillation columns with feed split (FS) configuration. The remainder of this paper is organized as follows. The Steady-State Design section describes the advantage of the heat-integrated configurations via quantitative analysis. The control structure design and controller design are presented in the Control section followed by rigorous nonlinear simulations for performance comparison. The conclusion is drawn in the final section.

STEADY-STATE DESIGN

Process Configuration and Design Procedure

At the steady-state design, a systematic procedure is employed to find the number of trays and feed tray location. For the single column configuration, initially the reflux

*Correspondence to: Dr C-C. Yu, Department of Chemical Engineering, National Taiwan University, Taipei 106-17, Taiwan.
E-mail: ccyu@ntu.edu.tw

ratio is set to 1.2 times of the minimum reflux ratio ($RR_{\min}$), then the number of trays and feed tray location are found by tray-by-tray calculation until the specification is reached, followed by refining the reflux ratio to meet the exact product specifications. For the heat-integrated systems, three configurations are considered: (1) feed split (FS), (2) light-split reserve (LSR), and light-split forward (LSF). Figure 1 shows these three configurations where one column is pressurized and the high pressure column provides the heat to boilup the vapour in the low pressure column via condensation. Theses three configurations differ in the direction of material flow versus the direction of the heat-integration. Again, the '1.2 $RR_{\min}$' criterion is used for the design of the heat-integrated column and 5% heat loss in the high pressure column is assume. That is heat transfer to the low pressure column via the heat exchange is limited to 95% of the heat of condensation in the high pressure column. Fifteen degrees of temperature driving force is assumed for heat transfer in all cases.

Steady-State Economics

Three systems are studied, they are: methanol–water, benzene–toluene, and isobutane–n–butane systems which correspond to high ($\alpha = 2.45–7.58$), medium ($\alpha = 2.35–2.65$), and low ($\alpha = 1.29–1.30$) relative volatilities, respectively. Table 1 compares the absolute energy consumption for these three chemical systems with three different feed compositions (of light component). The results show that percent energy saving ranges from 32–41% for the feed-split configuration, from 3–36% for the light-split forward configuration, and from 14–43% for the light-split reverse configuration. The percent of energy saving clearly reveals that the feed split configuration consistently provides economical incentives over the conventional single column configuration. However, the FS configuration show four product streams and, in the context of process control, this implies that we have a system with four controlled variables, quite possibly a 4×4 multivariable system. A possible tradeoff between steady-state economics and dynamical controllability may result as compared to the 2×2 multivariable system in the conventional configuration.

Table 1. Percentages of energy consumption (compared with the single column case as 100%) of various heat-integration configurations for different chemical systems with different feed compositions.

x_F	0.3	0.5	0.8
Methanol–water			
FS	68%	64%	62%
LSF	75%	67%	64%
LSR	70%	61%	57%
Benzene–toluene			
FS	66%	64%	61%
LSF	97%	81%	66%
LSR	86%	71%	59%
Isobutane–n–butane			
FS	60%	59%	59%
LSF	80%	75%	67%
LSR	77%	70%	60%

Figure 2 shows that the FS configuration is a typical parallel process where the products come from two parallel units and what we really care is the resultant composition after blending the product streams. That is, from a system perspective, we only need to control two product compositions, as opposed to the 4×4 control problem from the unit-wide perspective.

CONTROL

Nominal Operating Condition

A methanol–ethanol system is used to illustrate the control of heat-integrated system. The separation process separates 50/50 mixture of methanol and ethanol with top and bottom product specification of 99% methanol and 99% ethanol. All simulations were carried out using

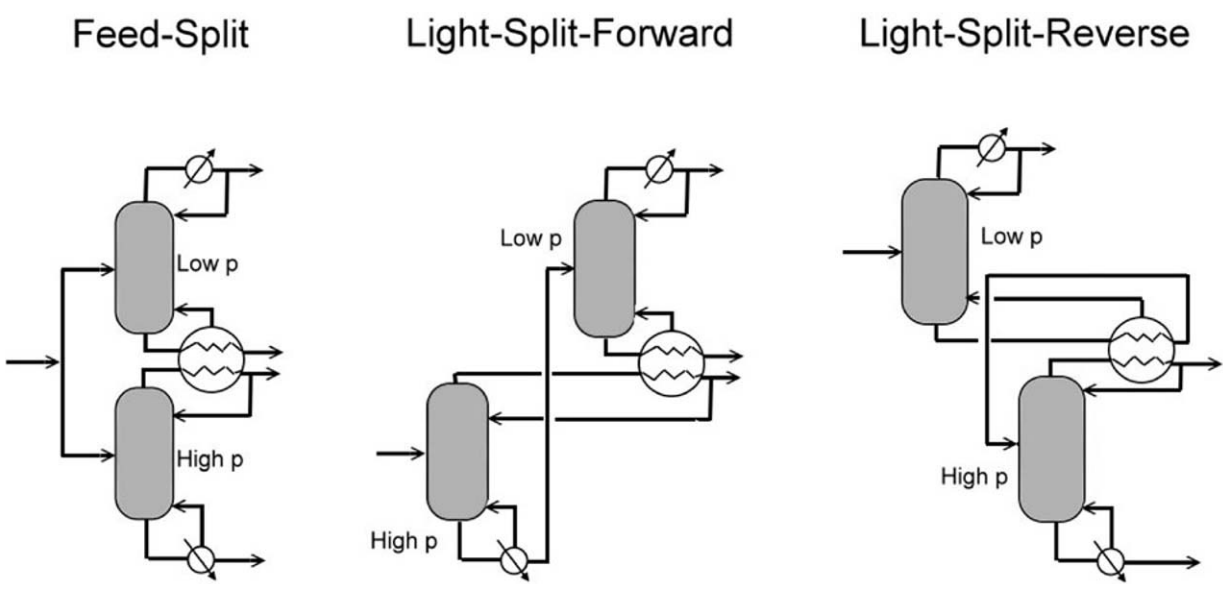

Figure 1. Three different heat-integration configurations.

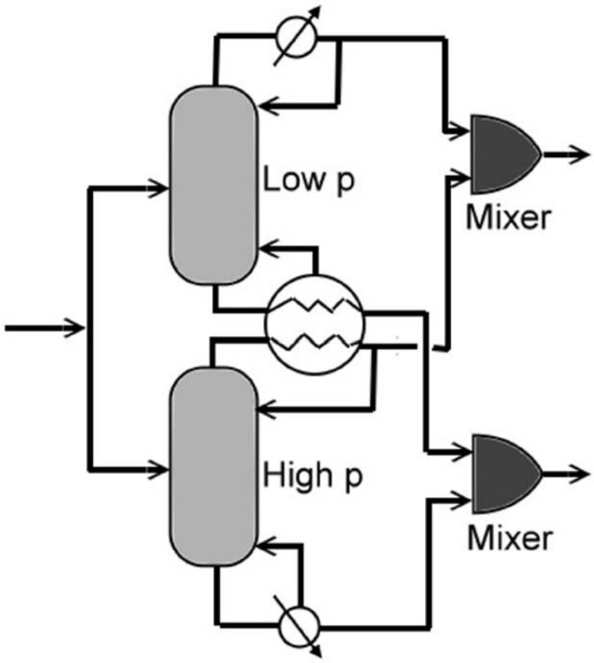

Figure 2. Treating the feed-split configuration as parallel units.

ASPEN Plus with the NRTL activity coefficient model to describe liquid phase nonideality. Steady-state economic analysis indicates that, again, the FS structure can save up to 49% as compared to 23% for the LSF and 24% for the LSR configurations (Table 2). Table 3 gives the nominal steady-state design with the low pressure column operated at 1 atm with 21 trays while the high pressure column is held at 3.5 atm with 35 trays. The heat input to the high pressure column is 107.3 kW which corresponds to a 49% energy saving as compared to the single column configuration which operated at 1 atm (208.1 kW). Figure 3 shows the process flowsheet with four product streams.

Control Structure Design

Two control structures are studied here. One is the conventional control structure for the heat-integrated column, called structure S-1 hereafter, and the other control structure treated the FS configuration is a parallel process which is denoted as structure S-2. As pointed out earlier, for the heat-integrated columns, we have only three control degrees of freedom (as opposed to four control degrees of freedom for two independent columns). For example, if the reflux-vapor boilup (RV) control structure is considered, these three possible manipulated variables are: reflux flows of high and low pressure column ($R_{F,L}$ and $R_{F,H}$) and the heat input to the high pressure column ($Q_{B,H}$). However, we have four controlled variables for structure S-1 and they are: $x_{D,H}$, $x_{B,H}$, $x_{D,L}$ and $x_{B,L}$ as shown in Figure 3. The additional control degree of freedom comes from the feed ratio to these two columns (FS_v) and, therefore, we have a 4×4 multivariable control problem. Once the controlled and manipulated variables are determined, the next step is to pair the input–output variables. One obvious choice is: $x_{B,H}$–$Q_{B,H}$, $x_{D,H}$–$R_{F,H}$, $x_{D,L}$–$R_{F,L}$ and $x_{B,L}$–FS_v (Figure 3). Actually, this is the control structure proposed by Chiang and Luyben (1988) when all four compositions are controlled.

Table 2. Percentages of energy consumption of various heat-integration configurations for methanol–ethanol systems ($F = 10$ kmol/h and $x_F = 0.5$).

Configuration	FS	LSF	LSR
% Energy consumption*	51.4	77.3	76.5

*Compared to single column case.

Table 3. Nominal steady-state for the methanol–ethanol heat-integrated columns.

	Value		Unit
Feed flow rate	10		*kmol/h*
Feed composition	0.5		*m.f. of methanol*
	HP col	LP col	
Top composition	0.99	0.99	*m.f.*
Bottoms composition	0.01	0.01	*m.f.*
Column pressure	1	3.5	*atm*
Tray pressure drop	0.0085	0.0085	*atm*
Total no. of trays	36	57	
Feed location	21	35	
Reboiler duty	107.3		*kW*
Approximated relative volatility	1.5 ~ 1.8	1.5 ~ 1.8	

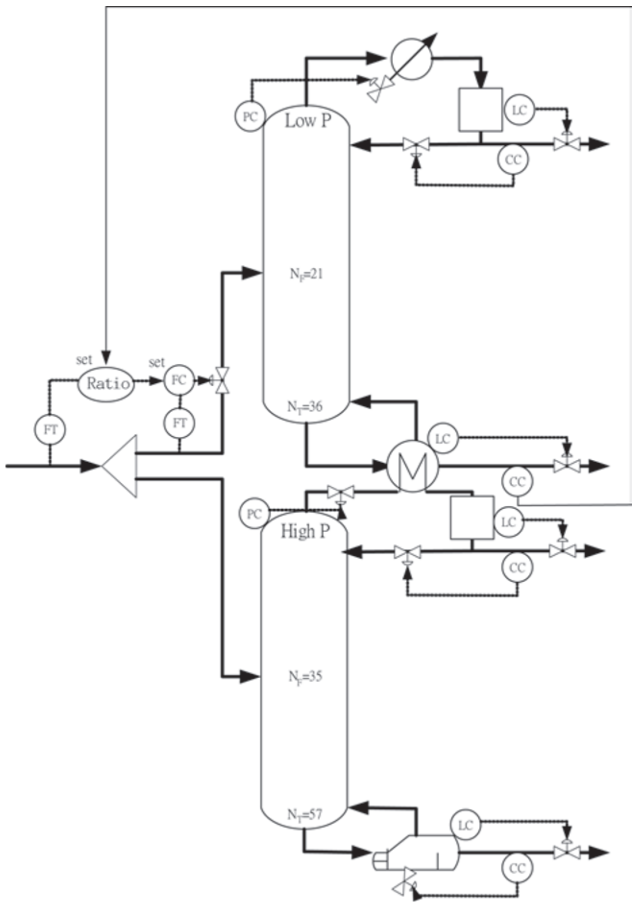

Figure 3. Conventional control structure for the FS configuration with control structure S-1.

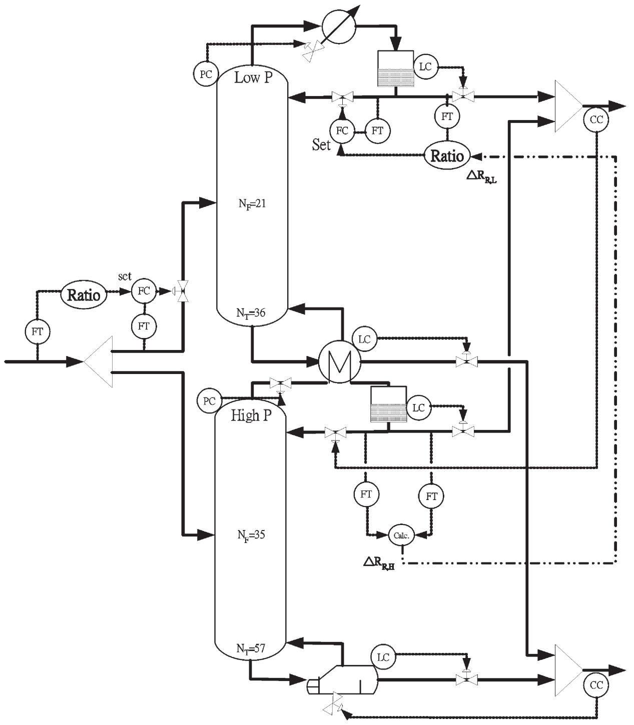

Figure 4. Treating the FS heat-integrated column in parallel topology with control structure S-2.

For the S-2 control structure, we have two controlled variables, the blended compositions of top and bottom products from high and low pressure different columns as shown in Figure 4. Thus, two of these four possible control degrees of freedom needed to be fixed. An obvious choice is to set the feed ratio (FS_v) at a constant value. This may lead to a suboptimal operating point as the feed composition changes. Figure 5 shows that when the feed composition varies from 0.1 to 0.8, the feed ratio falls between 0.52 and 0.55. Moreover, if one fix the feed ratio at 0.52, the optimality still can be achieved for $\pm 20\%$ feed composition changes. That implies little economic loss will be encounter when one choose to fix the feed ratio (FS_v). The second variable to be fixed is less obvious. The candidates are reflux ratio of the high or low pressure column (RR_H or RR_L) and the ratio of these two reflux ratios (RR_H/RR_L). Fixing the ratio of the reflux ratios is intuitively appealing because it seem to maintain the relative degree of fractionation in each unit. Once the two control degrees of freedom (FS_v and RR_H/RR_L) is fixed, we are left with two possible choices: $x_{B,mix}-Q_{B,H}$, $x_{D,mix}-R_{F,L}$ and $x_{B,mix}-Q_{B,H}$, $x_{D,mix}-R_{F,H}$. Here, the subscript mix stands for the mixed product composition. The later ($x_{B,mix}-Q_{B,H}$, $x_{D,mix}-R_{F,H}$ with a relative gain of 1.81) is selected because it is dynamically more favourable (the effects of manipulated variable propagate from the high pressure column to the low pressure one) (Figure 4).

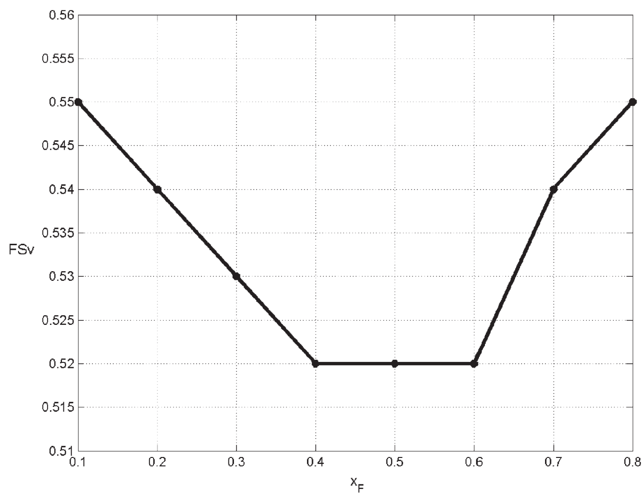

Figure 5. The optimal feed ratio for different feed composition.

Controller Design

For the control structure S-1, the 4×4 process transfer function matrix is obtained from step tests. First order responses were assumed and the process transfer function matrix becomes:

$$\begin{bmatrix} x_{D,L} \\ x_{B,L} \\ x_{D,H} \\ x_{B,H} \end{bmatrix} = \begin{bmatrix} \dfrac{2.49e^{-3s}}{264.8s+1} & \dfrac{0.44e^{-3s}}{307.4s+1} & \dfrac{0.21e^{-3s}}{834.1s+1} & \dfrac{-3e^{-3s}}{278.4s+1} \\ \dfrac{2.59e^{-3s}}{284.9s+1} & \dfrac{0.56e^{-3s}}{190.8s+1} & \dfrac{0.16e^{-3s}}{585.9s+1} & \dfrac{-3.55e^{-3s}}{294.6s+1} \\ 0 & \dfrac{-0.56e^{-3s}}{493.8s+1} & \dfrac{2.61e^{-3s}}{450.5s+1} & \dfrac{-1.93e^{-3s}}{311.4s+1} \\ 0 & \dfrac{-1.2e^{-3s}}{319.5s+1} & \dfrac{3.27e^{-3s}}{322.2s+1} & \dfrac{-6.59e^{-3s}}{390.6s+1} \end{bmatrix} \times \begin{bmatrix} R_{F,L} \\ FS_V \\ R_{F,H} \\ Q_{B,H} \end{bmatrix} \tag{1}$$

A three minute analyser dead time is added to each transfer function for the composition measurement. Corresponding relative gain array is:

$$\begin{array}{cc} & \begin{array}{cccc} R_{F,L} & FS_V & R_{F,H} & Q_{B,H} \end{array} \\ \Lambda = & \begin{bmatrix} 6.58 & -3.23 & -0.21 & -2.42 \\ -5.85 & 3.95 & 0.15 & 2.75 \\ 0 & -0.60 & 1.91 & -0.30 \\ 0 & 0.88 & -0.85 & 0.97 \end{bmatrix} \begin{array}{c} x_{D,L} \\ x_{B,L} \\ x_{D,H} \\ x_{B,H} \end{array} \end{array} \tag{2}$$

Next, sequential design is taken to find the tuning constants of the decentralized PID controllers (Huang *et al.*, 2003; Shen and Yu, 1994). That is an iterative procedure is taken and each controller is designed while rest of the loops are closed. In doing this, the closed-loop interaction is taken into account while maintaining the simplicity of single loop design. The controller parameters become:

$$\begin{aligned} &\text{loop 1}: K_c = 20.601 \quad && \tau_I = 74.77 \quad && \tau_D = 1.17 \\ &\text{loop 2}: K_c = 14.335 \quad && \tau_I = 105.58 \quad && \tau_D = 2.41 \\ &\text{loop 3}: K_c = 32.63 \quad && \tau_I = 70.25 \quad && \tau_D = 1.15 \\ &\text{loop 4}: K_c = -4.704 \quad && \tau_I = 144.15 \quad && \tau_D = 2.07 \end{aligned}$$

Because of its high dimensionality, a second set of tuning constants are obtained by reducing K_c to 60% and increasing reset time (τ_I) to 130% of their nominal values. For the control structure S-2, the 2×2 process transfer function matrix is also identified from step responses.

$$\begin{bmatrix} x_{D,mix} \\ x_{B,mix} \end{bmatrix} = \begin{bmatrix} \dfrac{3.06e^{-3s}}{347.4s+1} & \dfrac{-2.77e^{-3s}}{302.2s+1} \\ \dfrac{2.68e^{-3s}}{298s+1} & \dfrac{-5.42e^{-3s}}{366s+1} \end{bmatrix} \begin{bmatrix} R_{F,H} \\ Q_{B,H} \end{bmatrix} \tag{3}$$

This pairing gives a relative gain of 1.81. Again the sequential design approach is taken and PID settings become:

$$\begin{aligned} &\text{loop 1}: K_c = 20.75 \quad && \tau_I = 31.36 \quad && \tau_D = 1.198 \\ &\text{loop 2}: K_c = -12.34 \quad && \tau_I = 31.48 \quad && \tau_D = 1.197 \end{aligned}$$

Control Performance and Discussion

Dynamic simulations were performed to compare performance of these two control structures. All simulations were carried out in ASPEN Dynamics. The results indicate that for $\pm10\%$ feed composition changes, the simpler S-2 structure gives much better performance and the peak errors is consistently smaller than that of using control structure S-1 (Figure 6). It should be emphasized here that the control performance is actually evaluated according to the consistency in the closed-loop responses. Also note that two sets of tuning constants were evaluated under structure S-1: the tight tuning (S1-1) and loose tuning (S1-2). For $\pm10\%$ feed flow rate changes, the closed-loop responses of S-2 are comparable to that of the control structure S-1 as shown in Figure 7. The results presented here clearly

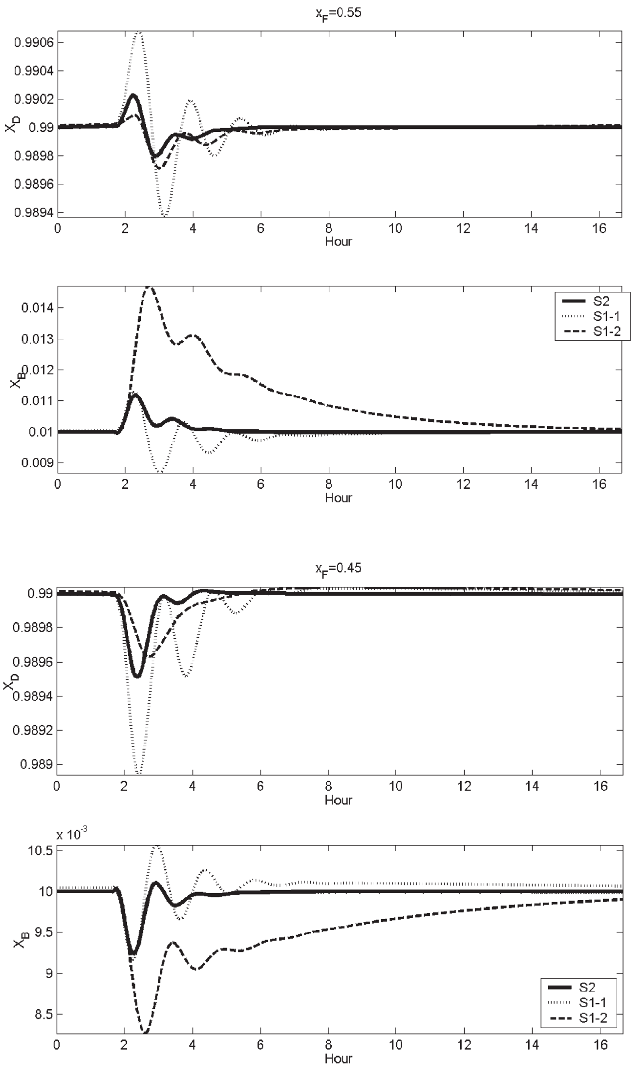

Figure 6. Responses for $\pm10\%$ methanol feed composition changes using control structures S-1 (tight tuning S1-1 and loose tuning S1-2) and S-2.

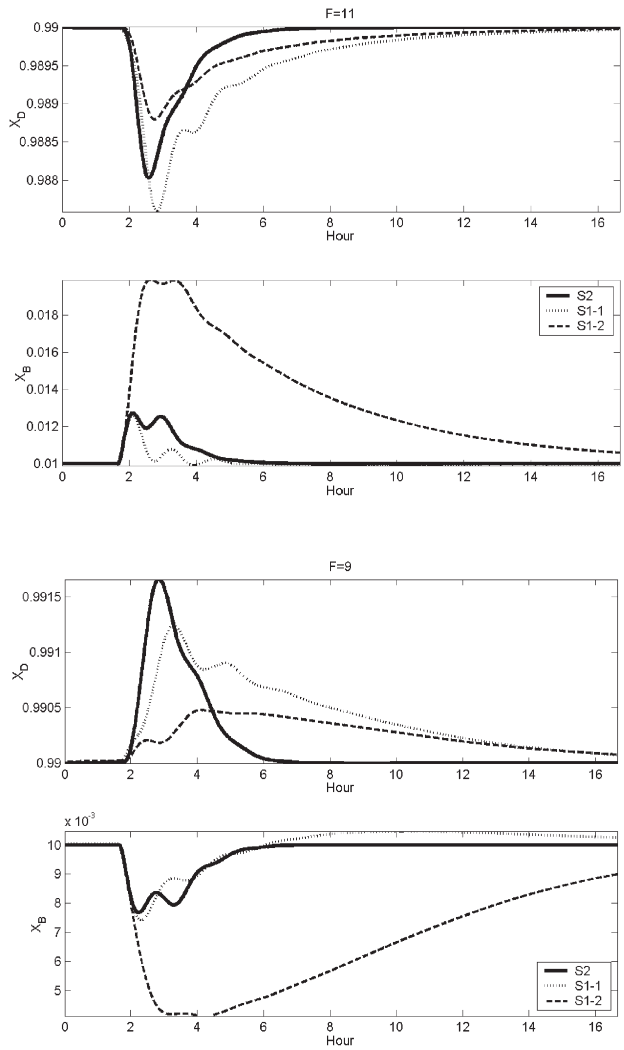

Figure 7. Responses for $\pm10\%$ feed flow rate changes using control structures S-1 (tight tuning S1-1 and loose tuning S1-2) and S-2.

show that more consistent control performance can be achieved using simpler control structure by taking the process topology into account. More importantly, for the heat-integrated columns, the improvement is obtained with virtually no loss in the economic objective (i.e., energy consumption).

The concept of treating the parallel units as a whole seems to offer an attractive alternative to control such processes. The advantages can be more evident if the number of units increases (Figure 8). Consider a process with n parallel unit (e.g., Figure 8). Immediately, this corresponds to a $n \times n$ multivariable system by keeping the output of n subunits on specification. Because we are only interested in the composition of the net output (this is especially true for plants making homogeneous products), the control system can be reduced to a SISO system (e.g., only one composition loop) with $n-1$ ratio loops. This simplifies the control system design (e.g., from $n \times n$ to 1×1) while maintaining comparable control performance. Still limitations are also observed for such a control strategy. An obvious one is that the ability to handle wide range of disturbances. Consider the feed split configuration with control structures S-1 and S-2. Based on dynamic simulations, the ranges of feed composition changes can be handled by S-1 and S-2 are $0.1 \le x_F \le 0.9$ and $0.2 \le x_F \le 0.8$, respectively. The reason is that the feed ratio is fixed for the structure S-2. A second potential problem is that it may become difficult to use the simple single temperature control for the structure S-2. That is composition control or some type of soft sensor should be used.

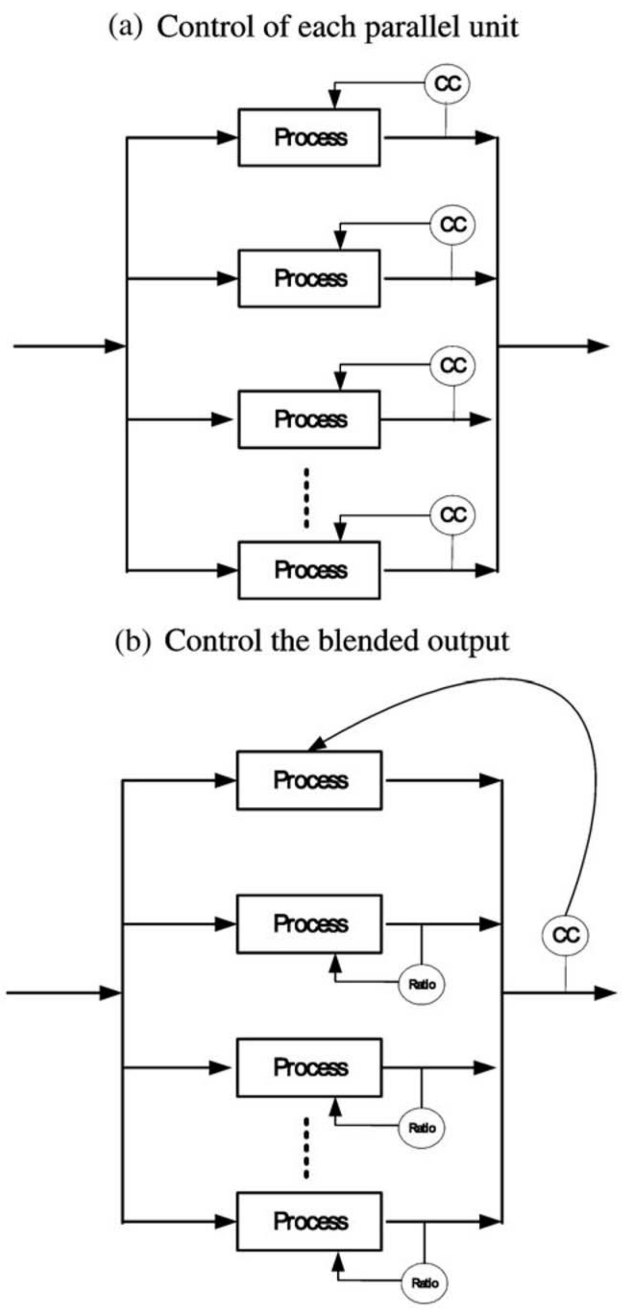

Figure 8. Conventional control structure (a) versus treating the parallel unit as a system (b).

CONCLUSION

Parallel processes are often encountered in process industries. In control system design, we can take advantage of this type of process topology. In this work, the control of parallel processes is illustrated with the heat-integrated distillation column example. The feed-split configuration is known to provide significant energy saving over the traditional single column configuration and it provides close to 50% energy saving over the system without heat-integration. However, the energy integration results in a highly interacting multivariable system with higher dimensionality and less control degrees of freedom. However, the parallel nature of the system leads to a completely different thinking of the control objective (as opposed to the conventional practice): control the global product composition at the end of the production line instead of the quality of each individual unit. This greatly simplifies the design procedure and subsequently results in a much simpler control system. The feed-split heat-integrated distillation example clearly shows that improved control performance can be achieved by taking the process topology into account. More importantly, this is obtained with much simpler hardware requirement as well as engineering manpower. The benefit can be much more substantial when the number of parallel units increases.

REFERENCES

Andrecovich, M.J. and Westerberg, A.W., 1985, A simple synthesis method based on utility bounding for heat-integrated distillation sequences, *AIChE J*, 31: 363.

Bildea, C.S. and Dimian, A.C., 1999, Interaction between design and control of a heat-integrated distillation system with prefractiontor, *Trans IChem, Part A, Chem Eng Res Des*, 77: 597.

Chiang, T.P. and Luyben, W.L., 1983, Comparison of energy consumption of five heat-integrated distillation configurations, *Ind Eng Chem Proc Des Dev*, 22: 175.

Chiang, T.P. and Luyben, W.L., 1988, Comparison of the dynamic performance of three heat-integrated distillation configurations, *Ind Eng Chem Res*, 27: 99.

Huang, H.P., Jeng, J.C., Chiang, C.H. and Pan, W., 2003, A direct method for multi-loop PI/PID controller design *J Process Control*, 13: 769.

King, C.J., *Separation Processes*, 2nd edition (1980) (McGraw-Hill, New York, USA).

Lin, S.W. and Yu, C.C., 2004, Interaction between design and control for recycle plants with heat-integrated separators, *Chem Eng Sci*, 59: 53.
Rix, A. and Gelbe, H., 2000, On the impact of mass and heat integration on design and control of distillation column Systems, *Trans IChemE*, *Part A*, *Chem Eng Res Des*, 78: 542.
Shen, S.H. and Yu, C.C., 1994, Use of relay-feedback test for automatic tuning of multivariable systems, *AIChE J*, 40: 627.
Tyreus, B.D. and Luyben, W.L., 1976, Dynamics and control of heat-integrated distillation columns, *Chem Eng Prog*, 72(9): 59.
Wang, S.J. and Lee, E.K., 2002, Nonlinear control of high-purity heat-integrated distillation system, *J Chem Eng Jpn*, 35(9): 848.
Weitz, O. and Lewin, D.R., 1996, Dynamic controllability and resiliency diagnosis using steady state process flowsheet data, *Comput Chem Eng*, 20: 325.
Yang, Y.H., Lou, H.H. and Huang, Y.L., 2000, Steady state disturbance propagation modelling of heat integrated distillation processes, *Trans IChemE, Part A, Chem Eng Res Des*, 78: 245.

ACKNOWLEDGEMENT

This work was supported by the Ministry of Economic Affairs under grant 92-EC-17-A-09-S1-019.

The manuscript was received 24 May 2004 and accepted for publication after revision 15 December 2004.